

# OBTAINING HIGHER LED'S LIGHTING CHROMATICITY AND LUMINOSITY WITH $\text{SiO}_2$ PARTICLES AT DIFFERENT DIAMETERS

Nguyen Doan Quoc Anh<sup>1</sup>, Sang Dang Ho<sup>1,\*</sup>, Phan Thi Minh Man<sup>1</sup>, Tran Khanh Duy<sup>1</sup>, Nguyen Thi Phuong Loan<sup>2</sup>

<sup>1</sup>Faculty of Electrical and Electronics Engineering, Ton Duc Thang University, Ho Chi Minh City, Vietnam.

<sup>2</sup>Faculty of Fundamental 2, Posts and Telecommunications Institute of Technology, Ho Chi Minh City, Vietnam.

\*Corresponding Author: Sang Dang Ho (email: hodangsang@tdtu.edu.vn)

(Received: 07-October-2024; accepted: 10-February-2025; published: 31-March-2025)

<http://dx.doi.org/10.55579/jaec.202591.476>

**Abstract.** This research delves into the promising applications of silicon dioxide ( $\text{SiO}_2$ ) nanoparticles related to their ability to enhance the conversion efficiency for luminescent materials through modifications in scattering effects. In addition, the study uses the semi-spherical lens packaging structure in preparing the light-emitting diodes (LED) models, owing to its advantages in achieving higher light extraction and minimal total internal reflection loss. The core objective of this paper is to augment existing knowledge by incorporating  $\text{SiO}_2$  nanoparticles uniformly into the silicone encapsulation of phosphor-converted white LEDs employing a semi-spherical lens (SSL) structure. The investigation includes the examination of the scattering coefficients through  $\text{SiO}_2$ -only samples with varying diameters of the nanoparticles, offering insights into the intrinsic properties of  $\text{SiO}_2$  in the context of LED encapsulation. Subsequently, the study explores the nuanced impact of  $\text{SiO}_2$ /phosphor layers on crucial LED performance metrics, including luminous efficacy, color rendering factor, and angular Correlated Color Temperature.  $\text{SiO}_2$  particle sizes ranging from 1 to 10 microns are

considered, revealing that  $\text{SiO}_2$  with specific radii contributes to discernible improvements in targeted LED lighting properties. These findings propel the exploration of  $\text{SiO}_2$ -enhanced LED technologies, introducing novel dimensions for optimizing efficiency and tailoring LED solutions to meet diverse lighting requirements, such as the combination of  $\text{SiO}_2$  and quantum dots or other phosphor materials for better optical properties in WLEDs or  $\text{SiO}_2$  integration in WLEDs for better thermal regulation approaches.

**Keywords:** Color rendering, Color uniformity, Lumen output, Scattering effects,  $\text{SiO}_2$ .

## 1. Introduction

In the dynamic landscape of solid-state lighting technology, the quest for high-brightness and highly efficient LEDs has gained considerable momentum [1–3]. The widespread application of lighting technology in displays, illumination,

and communication devices, has fueled intensive research in this domain [4]. Contemporary white LEDs typically employ a semiconductor chip emitting in the ultraviolet or blue wavelength range coupled with phosphors deposited in various configurations [5]. Despite their good photometric parameters, present LED-based devices face challenges, notably in luminous efficacy and light directionality due to the isotropic and incoherent nature of LED radiation [6–9].

Efforts to enhance device efficiency revolve around extracting wave-guided light trapped within LEDs and electroluminescent flat multilayer device structures [10]. Previous studies have explored surface modifications to improve light extraction and modify angular light intensity and/or spectrum [11–13]. Additionally, in the realm of phosphor-converted white LEDs, incorporating nanoparticles into the silicone encapsulant has demonstrated efficacy in improving efficiency [14, 15]. Noteworthy studies highlight the positive impact of  $ZrO_2$  and  $TiO_2$  nanoparticles on luminous efficacy. However, limitations related to the scattering ability of phosphors restraining light-extraction capabilities of nanoparticles have been identified.

Among various scattering-enhancement nanoparticles,  $SiO_2$  emerges as a significantly promising material with versatile applications in diverse fields, including biotechnology, agriculture, and optics. For example,  $SiO_2$  with different sizes was reported to enhance the conversion efficiency of solar cells via the changes in scattering effects [16]. Since  $SiO_2$  possesses particularly small thermal conductivity, below its counterparts, it does not conduct heat proficiently, and as such, benefits applications that require heat to be regulated. It can dissipate heat generated throughout device operation, sustaining the proficiency as well as durability for devices. Besides, while previous research has primarily focused on planar packaging structures, this study considers using the SSL packaging structure. The SSL structure, known for its advantages in higher light extraction and negligible total internal reflection loss, presents a promising approach for advancements in LED technology [17–19].

This paper endeavors to contribute to the existing knowledge by uniformly incorporating  $SiO_2$  nanoparticles into the silicone encapsulation of phosphor-converted white LEDs with an SSL structure. The investigation delves into the scattering coefficients of the encapsulation with only- $SiO_2$  samples. Subsequently, the study explores the impact of  $SiO_2$ /phosphor layers on luminous efficacy, color rendering factor, and angular Correlated Color Temperature (CCT) of the LEDs, considering varying  $SiO_2$  particle sizes (1-10 microns). The findings reveal that  $SiO_2$  with suitable radii contributes to improvements in specific LED lighting properties, such as possible  $SiO_2$  combination with other phosphor materials for better optical properties or better thermal regulation approaches using  $SiO_2$ .

## 2. Experimental

The yellow phosphor  $YAG : Ce^{3+}$  was prepared as follows. The solution consisting of starting materials  $Y_2O_3$ ,  $\alpha-Al_2O_3$ , and  $CeO_2$  were produced by mixing the ingredients in nitric acid. Then, this mixture was heated at  $105\ 0^C$  to produce a precursor. The precursor was subsequently burned at  $1500\ 0^C$  for three hours in a reducing air environment [20, 21]. The  $SiO_2$  nanoparticles with various radii, bought from Aladdin Co., were mixed with  $YAG : Ce^{3+}$  (YAG:Ce) phosphor and silicone. For the preparation of the LED model (shown in Fig. 1), the SSL structure was selected, featuring a polycarbonate lens with a diameter of 12 mm and a height of 6 mm (Figs. 1a and 1b). A cluster of nine square blue chips, integral to this structure (Fig. 1c), adopts a horizontal configuration with dimensions of  $1.14 \times 0.1$  mm, emitting light with a wavelength centered at 453 nm. To achieve a homogenous structure, a prepared slurry is injected into the lens to fill the gap. Subsequently, the devices undergo curing in an oven set at  $60\ 0^C$  for 2 hours, finalizing the manufacturing process. Optical performance evaluations are conducted utilizing an integrating sphere system to comprehensively assess the characteristics of the SSL-structured LEDs [22].

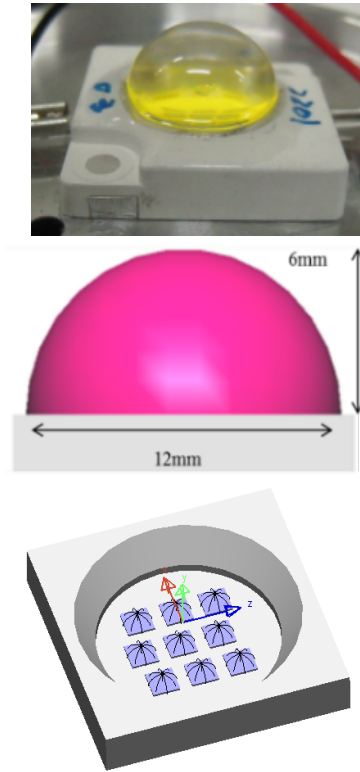


**Fig. 1:** White LED modelling: (a) Prepared LED package, (b) Simulation of WLEDs using LightTools, and (c) Simulation of wire-bonded chip cluster.

### 3. Results and discussion

The scattering efficiency of light with the  $SiO_2$  films featuring different  $SiO_2$  particle radii is presented in Fig. 2. Fig. 2a is the data collected with 1-5 microns  $SiO_2$  particles while Fig. 2b the particle radius ranges from 6 microns to 10 microns. In all figures, the scattering factor increasing with larger  $SiO_2$  radius, especially with in the ultraviolet and blue radiation wavelengths (380-480nm). Besides, the scattering enhancement among 1-5 microns of  $SiO_2$  radius is fairly greater than that among larger radii.

The greater scattering coefficients will support the blue light absorption and conversion of the luminescent-converter film (LCF). As a result, the intensity of optical power of different light bands varies, as depicted in Fig. 3. As can be interpreted from the figure, the blue emission band (455 nm) is lower than that of the yellow-red band (525-600 nm). Moreover, in-

creasing the particle size of  $SiO_2$  seems to have no significant impact on the overall intensity of the optical power of the as-prepared LED package. The differences in optical strength between two light emission band can be attributed to the scattering effects of the  $SiO_2$  nanoparticles. In the presence of  $SiO_2$  nanoparticles, more incident lights are scattered and traverse around the nanoparticles, leading to the greater probability of light absorbed and converted by the phosphor around the  $SiO_2$ . Thus, the greater peak centered at  $\sim 575$  nm is probably originated from the yellow phosphor  $YAG : Ce^{3+}$ , indicating the noticeable conversion efficiency by the phosphor via the mean of scattering by  $SiO_2$  nanoparticles [23].

The improve conversion factor can contribute to heightening the lumen efficiency of the LED. In Fig. 4, the lumen output of the LED package is demonstrated with different  $SiO_2$  particle radii within 1-10 microns. It shows that the highest lumen intensity of  $\sim 74$  lm is obtained when  $SiO_2$  radius reaches 3 microns. Beyond that particle size, the lumen output slightly decreases but is quite stable around 73.3 lm, greater than the value recorded with 1-2 microns of  $SiO_2$  diameters.

Considering that the concentrations of the phosphor and the  $SiO_2$  are fixed, increasing the diameter of  $SiO_2$  nano-spheres can reduce the void numbers between the phosphor and the  $SiO_2$ , increasing the interaction between the nanoparticles and the blue light. Therefore, the blue light will propagate in a longer path and be absorbed more effectively by the phosphor, leading to the greater intensity of the luminescent light power. On the other hand, the smaller  $SiO_2$  particles will result in the greater presence of voids in the film, and the blue-light scattering is weaker, causing the lower blue-light utilization efficiency by the phosphor. Besides, when the  $SiO_2$  particle size increases beyond a certain number, which is 3 microns in this paper, the power of lumen output decreases as a result of increasing substrate-absorbed blue light by back-scattering [24–26]. The scattering enhancement by  $SiO_2$  addition can result in the lower CCT levels as the blue light intensity by LED chip declines. The obtained CCT range for the prepared LED with different  $SiO_2$  radii

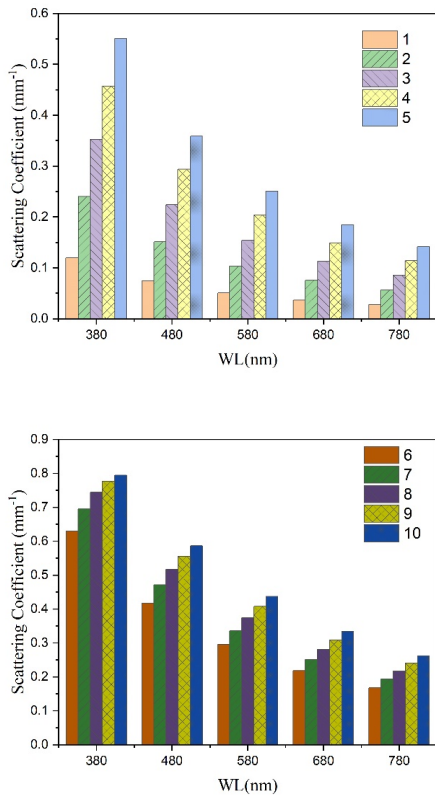


**Fig. 2:** The scattering efficiency with different  $SiO_2$  radii: (a) 1-3 microns and (b) 6-10 microns.

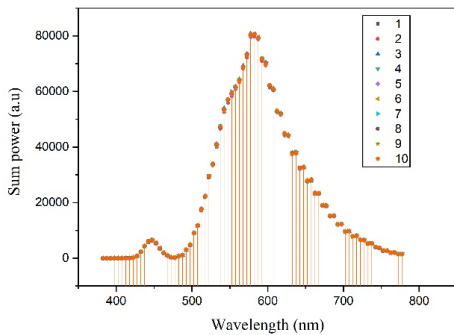


**Fig. 3:** The optical power of the luminescent-converter film on increasing  $SiO_2$  particle sizes.

is around 2977-3050 K, which is considered as warm white light. The variation of CCT range among different  $SiO_2$  radii is depicted in Fig. 5, in which the data for 1-5 microns is in Fig. 5a

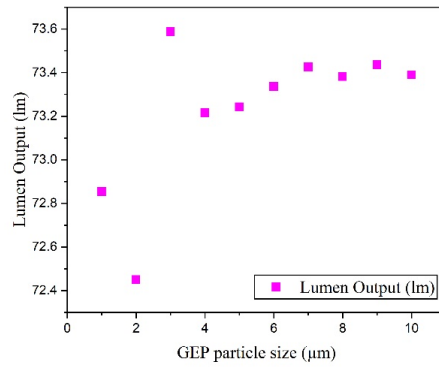


**Fig. 4:** The power of lumen output from LEDs with different  $SiO_2$  radii.

and 6-10 microns is in Fig. 5b. With increasing particle size of  $SiO_2$ , the variance between angular CCT values become less severe, owing to the scattering effects. The color deviation or delta-CCT with different  $SiO_2$  radii is shown in Fig. 6. A noticeable fluctuation of delta-CCT level is observed. The most notable increase of delta-CCT is noted with 2-micron  $SiO_2$  particles. Further increasing  $SiO_2$  diameters leads to the lower delta CCT but still larger than the value obtained with 1-micron  $SiO_2$ . However, the lowest color deviation is collected when the  $SiO_2$  nanoparticle size reaches 8 microns, indicating the best color distribution uniformity of the white LED output. With the enhancement in scattering factor by larger  $SiO_2$  size, the blue-light direction is adjusted to the larger angle, allowing it to reach the phosphor particles in the edge of the layer, supporting the light distribution at the margin of the package. Thus, the color difference between the side and direct viewing angles is significantly reduce, resulting in greater color uniformity.

Subsequently, the colour rendering performance is considered to further assess the effect of  $SiO_2$  particle size on the LED output quality. The colour rendering index CRI and colour quality scale CQS are evaluated. The CRI factor is demonstrated in Fig. 7 and the CQS is depicted in Fig. 8. In general, findings show that the  $SiO_2$  can support the colour rendering improvement. In particular, the CRI and CQS show different trends. The CRI fluctuates among the

$SiO_2$  radii, peaking at 56.26 with 4-micron  $SiO_2$  radius and bottoming out at 56.16 with 6-micron  $SiO_2$  radius. Meanwhile, the CQS values shows a gradual increase and reach a peak with 5-micron  $SiO_2$  radius before showing a small decline as the  $SiO_2$  radius continuously increases. In this case, determining which particle size of  $SiO_2$  is optimal could be based on the CQS rather than the CRI. It is because the CQS is a parameter developed to overcome the drawbacks of CRI. The CRI has limited colour samples to evaluate and does not consider colour saturation. The CQS, on the other hand, assesses a larger amount of colour samples and also colour saturation of the tested white light sources. Additionally, the CQS covers the rendering index, the human visual orientation, and the colour coordinates. Therefore, the evaluation made with CQS can be more accuracy. Thus, increasing the  $SiO_2$  radius potentially enhances the colour reproduction efficiency, and the optimal  $SiO_2$  radius for the greatest enhancement in chromatic rendition in this work should be 5 microns.

## 4. Conclusion

In conclusion, this research sheds light on the multifaceted applications of silicon dioxide ( $SiO_2$ ) nanoparticles, particularly their capacity to enhance the conversion efficiency of luminescent materials by scattering effects. The utilization of the semi-spherical lens packaging structure (SSL) in the preparation of LED models proves to be a strategic choice, leveraging its inherent advantages in achieving higher light extraction and minimizing total internal reflection loss. The luminous efficacy, color rendering factor, and angular CCT of the white LED are examined with different  $SiO_2$  radii, ranging from 1 to 10 microns. The increasing  $SiO_2$  particle sizes leads to the enhancement in scattering of blue light, showing the higher blue-light utilization efficiency. The optical power shifts to the yellow emission band as the blue light is effectively absorbed and converted by the phosphor, attributed to the scattering improvement by  $SiO_2$ . The increase in  $SiO_2$  radius does benefits the chromatic performance and lumen output of the LED. Suitable  $SiO_2$  sizes should be

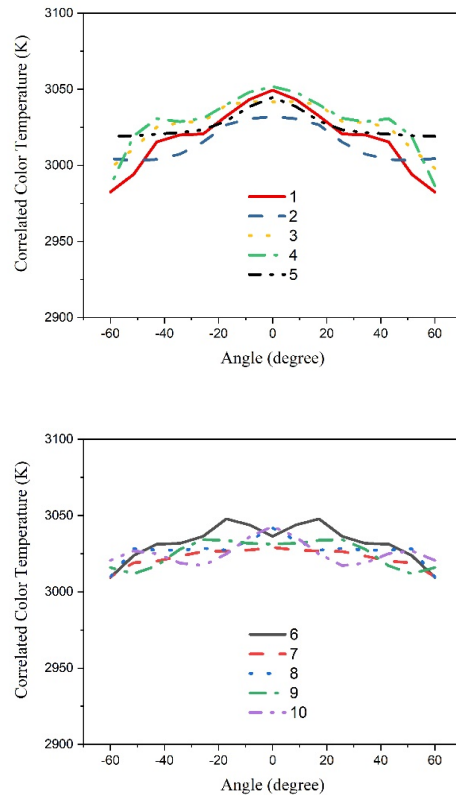


**Fig. 5:** Angular CCTs with different  $SiO_2$  radii: (a) 1-3 microns and (b) 6-10 microns.

chosen based on the priority of the light features. 4-5 microns are the optimal  $SiO_2$  radii for high color rendition performance. 3 microns of  $v$  yields the highest lumen output. 8 microns of  $SiO_2$  diameter results in the lowest color variation, meaning the highest color-distribution uniformity. The demonstrated enhancements in LED performance underscore the potential of  $SiO_2$  nanoparticles as a valuable component in advancing the efficiency and customization of LED lighting technologies for further innovation in the field.

## References

- [1] H.T. Tung, N D.Q. Anh, and H.Y. Lee. Impact of phosphor granule magnitudes as well as mass proportions on the lumi-

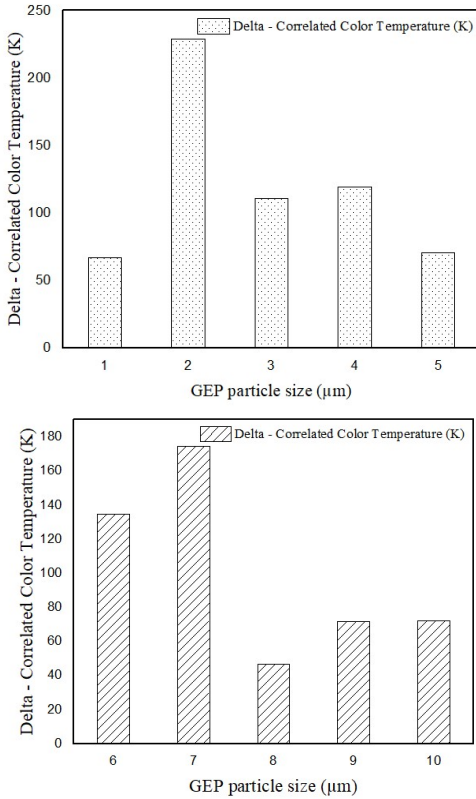


Fig. 6: Chromatic deviation with different  $SiO_2$  radii: (a) 1-3 microns and (b) 6-10 microns.

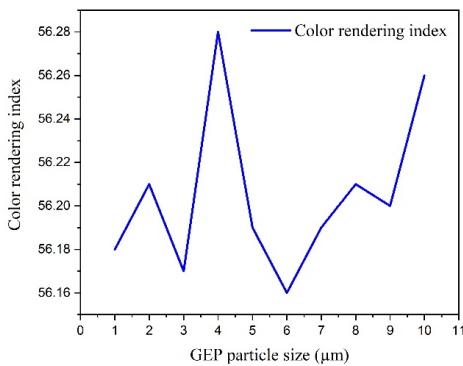


Fig. 7: Color rendering index with different  $SiO_2$  radii.

nous hue efficiency of a coated white light-emitting diode and one green phosphor film. *Optoelectron. Adv. Mater. - Rapid Commun.*, 18(1-2):58-65, 2024.

[2] V.T. Pham, N.H. Phan, G.F. Luo, H.Y.

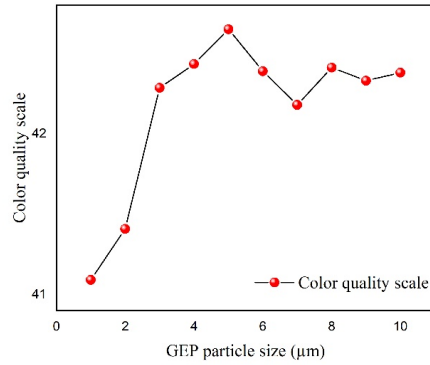


Fig. 8: Color quality scale with different  $SiO_2$  radii.

Lee, and D.Q.A. Nguyen. The application of calcium carbonate  $caco_3$  and titania  $tio_2$  for color homogeneity and luminous flux enhancement in pc-leds. *J. Adv. Eng. Comput.*, 5(2):75, 2021.

[3] N.H.S. Dang, D.M.T. Nguyen, T.P.L. Nguyen, D.Q.A. Nguyen, and H.Y. Lee. Enhance wleds performance with additional phosphor materials in multi-layer remote structure. *J. Adv. Eng. Comput.*, 5(3):167, 2021.

[4] N.D.M. Thong, D.N.H. Son, S.D. Ho, N.D.Q. Anh, and H.Y. Lee. The use of  $y_3al_5o_{12}:ce_3+$  and  $catio_3:pr_3+$  in a dual-layer remote phosphor configuration improves the optical efficiencies of a phosphor-in-glass white light-emitting diode. *J. Adv. Eng. Comput.*, 6(1):36, 2022.

[5] C. Polzer et al. Correlative two-color two-photon (2c2p) excitation sted microscopy. *Biomed. Opt. Express*, 9:4516, 2019.

[6] M.M. Magno-Canto, L.I.W. McKinna, B.J. Robson, and K.E. Fabricius. Model for deriving benthic irradiance in the great barrier reef from modis satellite imagery. *Opt. Express*, 27:A1350, 2019.

[7] R. Hirayama, H. Nakayama, A. Shiraki, T. Kakue, T. Shimobaba, and T. Ito. Projection of multiple directional images on a volume structure with refractive surfaces. *Opt. Express*, 27(20):27637, 2019.

- [8] D. Durmus and W. Davis. Blur perception and visual clarity in light projection systems. *Opt. Express*, 27(4):A216, 2019.
- [9] J. J. Gómez-Valverde et al. Automatic glaucoma classification using color fundus images based on convolutional neural networks and transfer learning. *Biomed. Opt. Express*, 10(2):892, 2019.
- [10] Q. Zaman et al. Two-color surface plasmon resonance nanosizer for gold nanoparticles. *Opt. Express*, 27(3):3200, 2019.
- [11] M. R. Edwards et al. A multi-terawatt two-color beam for high-power field-controlled nonlinear optics. *Opt. Lett.*, 45(23):6542, 2020.
- [12] R.E. O’Shea, S.R. Laney, and Z. Lee. Evaluation of glint correction approaches for fine-scale ocean color measurements by lightweight hyperspectral imaging spectrometers. *Appl. Opt.*, 59(7):B18, 2020.
- [13] L.M. Lozano et al. Optical engineering of polymer materials and composites for simultaneous color and thermal management. *Opt. Mater. Express*, page 1990, 2019.
- [14] H. Von-Breymann and E. Montenegro-Montenegro. Validation of a scale to measure perceived residential environment quality in a latin american setting / validación de una escala para medir la percepción de la calidad del entorno residencial en un contexto latinoamericano. *PsyEcology Biling. J. Environ. Psychol.*, 10(2):217–256, 2019.
- [15] E. Bijanzadeh, V. Barati, Y. Emam, and M. Pessarakli. Assessment of the crop water stress index and color quality of bur clover (*medicago polymorpha* l.) under different irrigation regimes. *Commun. Soil Sci. Plant Anal.*, 50(22):2825–2835, 2019.
- [16] T. Parczewska. The quality of care for 5–9-year old children in the school environment in poland measured with the use of the sacers scale. *Educ. 3-13*, 48(5):541–549, 2019.
- [17] T. Fukuda, K. Takamatsu, T. Bamba, and E. Fukusaki. Potato tuber metabolomics-based prediction of chip color quality and application using gas chromatography/flame ionization detector. *Biosci. Biotechnol. Biochem.*, 84(11):2193–2198, 2020.
- [18] X. Soria-Perpinya, V. Sancho-Tello, M. J. Rodriguez, C. Duran, J. M. Soria, and E. Vicente. Influence of chlorophyllaquantification methods in ecological quality indices. <https://www.unb.ca/cic/research/applications>, 9(1):104–112, 2019.
- [19] S. Daneshvar and K. A. Adesina. Modified variable return to scale back-propagation neural network robust parameter optimization procedure for multi-quality processes. *Eng. Optim.*, 51(8):1352–1369, 2018.
- [20] S. Spitzer-Shohat, M. Goldfracht, C. Key, M. Hoshen, R. D. Balicer, and E. Shadmi. Primary care networks and team effectiveness: the case of a large-scale quality improvement disparity reduction program. *J. Interprofessional Care*, 33(5):472–480, 2018.
- [21] R. A. Reyes-Villagrana et al. High-intensity ultrasonication of rabbit carcasses: a first glance into a small-scale model to improve meat quality traits. *Italian J. Animal Sci.*, 19(1):544–550, 2020.
- [22] S. Simonsen, S. Juul, M. Kongerslev, S. Bo, E. Folmo, and S. Karterud. The mentalization-based therapy adherence and quality scale (mbt-aqs): Reliability in a clinical setting. *Nord. Psychol.*, 71(2):104–115, 2018.
- [23] A. Shelestov et al. Essential variables for air quality estimation. *Int. J. Digit. Earth*, 13(2):278–298, 2019.
- [24] X. Cao, M. Zhang, A. S. Mujumdar, and Z. Wang. Effect of microwave freeze-drying on microbial inactivation, antioxidant substance and flavor quality of ashitaba leaves (*angelica keiskei koidzumi*). *Dry. Technol.*, 37(6):793–800, 2018.
- [25] D. Vazquez-Sanchez, E.E.S. Garcia, J. A. Galvao, and M. Oetterer. Quality index method (qim) scheme developed for

whole Nile tilapias (*Oreochromis niloticus*) ice stored under refrigeration and correlation with physicochemical and microbiological quality parameters. *J. Aquat. Food Prod. Technol.*, 29(3):307–319, 2020.

- [26] H.T. Tung, B.T. Minh, N.L. Thai, H.Y. Lee, and N.D.Q. Anh. ZnO particles as scattering centers to optimize color production and lumen efficiencies of warm white LEDs. *Optoelectron. Adv. Mater. - Rapid Commun. - OAM-RC*, 18(5-6):283–288, 2024.

## About Authors

**Nguyen Doan Quoc ANH** was born in Khanh Hoa province, Vietnam. He has been working at the Faculty of Electrical and Electronics Engineering, Ton Duc Thang University. Quoc Anh received his PhD degree from National Kaohsiung University of Science and Technology, Taiwan in 2014. His research interest is optoelectronics. He can be reached via email: nguyendoanquocanh@tdtu.edu.vn.

**Sang Dang HO** was born in Ho Chi Minh City, Vietnam in 1973. He received the M.Ss. degree in Electrical Engineering from Ho Chi Minh University of Technology, Ho Chi Minh City, Vietnam in 2008, and received the Ph.D. degree in Electrical Engineering from VSB-Technical University of Ostrava, Czech Republic, in 2020. Presently, he is working as a lecturer at the Faculty of Electrical and Electronics Engineering, Ton Duc Thang University, Ho Chi Minh City,

Vietnam. His research interests involve the optimization of the power system and applications of soft computing in control of electric machine drives and optics science. He can be reached via email: hodangsang@tdtu.edu.vn.

**Nguyen Thi Phuong LOAN** was born in Da Nang province. In 2006, she received her master degree from University of Natural Sciences, and received the Ph.D. degree in Electrical Engineering from Ton Duc Thang University, in 2024. Her research interest is optoelectronics. She has worked at the Faculty of Fundamental 2, Posts and Telecommunications Institute of Technology, Ho Chi Minh City, Vietnam. She can be reached via email: ntploan@ptithcm.edu.vn.

**Phan Thi Minh MAN** was born in Ho Chi Minh city, Vietnam. She has been studying at the Faculty of Electrical and Electronics Engineering, Ton Duc Thang University. Her research interest is optoelectronics and lighting design. She can be reached via email: 422H0012@student.tdtu.edu.vn.

**Tran Khanh DUY** was born in Long An province, Vietnam. He has been studying at the Faculty of Electrical and Electronics Engineering, Ton Duc Thang University. His research interest is optical science and power system. He can be reached via email: 42000642@student.tdtu.edu.vn.